ESOMAT 2009, 02001 (2009)
DOI:10.1051/esomat/200902001

Isotropic Phase Transformation in Anisotropic Stainless Steel 301LN Sheets

A.M. Beese[a,1], D. Mohr[1,2] and P.-O. Santacreu[3]

[1] Impact and Crashworthiness Laboratory, Department of Mechanical Engineering, Massachusetts Institute of Technology, Cambridge MA, USA
[2] Solid Mechanics Laboratory (CNRS-UMR 7649), Department of Mechanics, École Polytechnique, Palaiseau, France
[3] ArcelorMittal R&D, Isbergues, France

Abstract. The phase transformation due to mechanical loading in cold-rolled stainless steel 301LN sheets is investigated experimentally. A series of uniaxial tension experiments is performed to quantitatively investigate the effect of initial anisotropy on the martensitic transformation kinetics. Three methods are employed to measure the martensite content: (1) micrography, (2) global magnetic saturation, and (3) local magnetic induction. The first two methods require interrupted tests, while the third method allows for the in-situ detection of the evolution of the martensite volume ratio. All three methods are able to detect the increasing martensite content with plastic strain, and in addition they show that the rate of austenite-to-martensite transformation is not loading direction dependent. In particular, the local magnetic induction technique appears to be sufficiently sensitive to detect these relative differences. The results show that micrography has limited accuracy in quantifying the absolute martensite content due to material preparation. However, the global magnetic method is deemed to be an accurate method to quantify the absolute martensite content, and measurements using this method can be used to calibrate the local magnetic induction method for in-situ monitoring of martensite content evolution. In addition, it was determined that the martensite evolution in this textured material has no directional dependence.

1. INTRODUCTION

It is well known that austenitic stainless steels may undergo phase transformation from austenite to martensite when subjected to mechanical or thermal loading [1-3]. The present paper is concerned with an anisotropic stainless steel 301LN alloy which features strain-induced nucleation at temperatures between -60°C and 83°C [4]. In particular, temper-rolled sheets are studied, which have a tensile strength of about 1000 MPa, and an initial martensite content of about 24%-vol. Transformation kinetics laws are used to describe the evolution of the martensite content. Olson and Cohen [3] developed an isotropic transformation kinetics law for strain-induced nucleation that expresses the martensite content as a function of plastic strain and temperature. Stringfellow et al. [5] expanded this isotropic law by incorporating a term that accounts for the pressure-dependence of the martensitic transformation. With the goal of developing a constitutive model for the large deformation behavior of stainless steel 301LN, the martensitic transformation kinetics are experimentally examined. In order to accurately define a transformation kinetics law, several techniques to quantify the evolution of martensite during loading are investigated. Micrography and global magnetic saturation require interrupted tests (i.e. the extraction of small samples), while the local magnetic permeability measurements allow for the in-situ monitoring of the martensite content evolution during tests.

2. MEASUREMENT TECHNIQUES

Many techniques for quantifying the amount of martensite and austenite in stainless steels have been investigated in the literature, including neutron diffraction, density measurements, scanning electron microscopy, Moessbauer spectroscopy, X-ray diffraction, optical metallography and magnetization measurements [6-9]. Here, the two

[a] e-mail : abeese@mit.edu

Article available at http://www.esomat.org or http://dx.doi.org/10.1051/esomat/200902001

latter experimental techniques are considered to quantify the evolution of martensite in samples extracted from stainless steel 301LN tensile specimens.

2.1 Micrography

In micrographical analysis, the individual phases are distinguished with respect to their emissivity (or reflectivity), and therefore, the specimen surface preparation plays an important role. The phase distribution at the specimen surface must be representative of the bulk material since the measured phase area fractions are assumed to be identical to the phase volume fractions. This poses a particular challenge in materials that are prone to phase transformations throughout the machining and polishing of the specimen surface.

We embed the specimen in an epoxy and apply a standard polishing procedure using sandpaper and diamond paste with $1\mu m$ diameter grit particles. Beraha's tint ($50ml$ H_2O, $10ml$ HCl, $0.15g$ $K_2S_2O_5$) is used to etch each polished specimen surface. This procedure is recommended [10] to increase the difference in appearance of the martensite with respect to the austenite. Micrographs are taken using a digital camera mounted on a compound microscope (Zeiss Axioplan Optical Microscope, Zeiss AxioCam MRc 5 camera). The photographs are acquired at a resolution of 1300 x 1200 pixels in the Tagged Image File Format (TIFF). The image processing module of the software Matlab is subsequently used to determine the image area fractions for different gray scale intervals.

2.2 Global magnetic saturation method using a sigmameter

The austenitic and martensitic phases in stainless steel feature very different magnetic properties. Martensite is ferromagnetic while austenite is paramagnetic. Since stainless steel 301LN is almost entirely comprised of these two phases (with only 1-3% of a magnetic ferrite phase), examining the evolution of the magnetic properties of a specimen allows for the determination of the martensite content. The saturation induction is an intrinsic material property which depends only on the chemistry and crystal structure [11, 12]. Saturation induction measurements may be performed using a so-called sigmameter. A small cubic sample with a side length of less than $5mm$ is fully enclosed in the measurement chamber. The sample is progressively magnetized by increasing the surrounding magnetic field to about $100kA/m$. The saturation induction, B_S, of the multi-phase material is then determined from the measured magnetic field, H_S, and sample saturation magnetization, M_S (e.g. [12]),

$$B_S = H_S + 4\pi M_S \,. \tag{1}$$

Knowing the saturation induction of α'-martensite, $B_S^{\alpha'}$, the martensite volume fraction, $f_{\alpha'}$, may be determined from the rule of mixtures,

$$f_{\alpha'} = \frac{B_S}{B_S^{\alpha'}} \,. \tag{2}$$

All saturation induction measurements have been performed by ArcelorMittal. It is emphasized that this method measures the average properties throughout the entire sample volume which reduces possible measurement errors related to surface effects.

2.3 Local magnetic induction method using a ferritescope

The ferritescope provides an in-situ method for the measurement of the martensite content. The ferritescope is a commercially available measurement device that has been developed for the measurement of the ferrite content in austenitic and duplex steels. A low frequency alternating magnetic field is generated around a cylindrically shaped iron probe (5mm diameter). A coil wound around this probe is used to measure changes in the surrounding magnetic field due to the presence of the sample. There is a linear relationship between the output voltage (amplified eddy current) and the magnetic permeability of the sample. As with the magnetic saturation measurements, the magnetic permeability measurement can then be related to the martensite content through the rule of mixtures.

The proportionality factor between the ferritescope output signal and the martensite content depends on the position of the probe with respect to the sample and the sample thickness. Throughout our measurements, the probe is perpendicular to the specimen surface (and always in direct contact with the specimen surface). The ferritescope manufacturer provides a set of thickness correction curves that describe the effect of the specimen thickness on the ferritescope measurements [13]. Denoting the current specimen thickness in *mm* as t and the dimensionless device output signal as S_t, we approximate the thickness correction factor, χ_t, through the following empirical relationship

$$S_0 = \chi_t \cdot S_t \quad \text{with} \quad \chi_t(S_t,t) = \begin{cases} 1 - 0.008t + (0.0804 - 0.0017S_t)t^{-1.25} & \text{for } t < t_0 \\ 1 & \text{for } t > t_0 \end{cases} \tag{3}$$

where $t_0 = t_0(S_t)$ is the maximum thickness for which the measured signals are thickness dependent ($\chi_t > 1$); and S_0 is the corresponding thickness-independent signal value. The proportionality factor $\alpha_f = 1.67$ relating S_0 of an unstressed specimen to the martensite volume percent, $f_{\alpha'}$, has been calibrated from comparison with sigmameter measurements (Fig. 1).

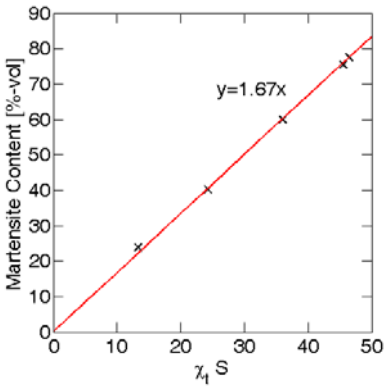

Fig. 1. Calibration curve between sigmameter absolute measurements and ferritescope measurements (symbols are data points, and the solid line gives the calibration factor 1.67).

3. EXPERIMENTS AND EVALUATION

3.1 Uniaxial tensile testing

Uniaxial tensile tests are performed on specimens with a gage width of 20*mm*, a gage length of 50*mm*, and a thickness of 1.52*mm*. Four specimens are extracted such that their tensile direction is aligned with each of the following material directions: rolling (0°), 45°, and cross (90°). A thermocouple attached to the gage section confirms isothermal conditions, as there was very little temperature increase (about 5°C) during each test. Specimens are loaded in tension under displacement control, with an actuator velocity of 0.5*mm/min*, corresponding to a plastic strain rate between 1.4 x 10^{-4}/*s* and 1.8 x 10^{-4}/*s*.

The resulting uniaxial stress-strain curves are given in Fig. 2. Depending on the direction of loading, the initial yield stress is different (σ_y=876*MPa* in the material rolling direction, and 913*MPa* in the material cross and 45° directions). Even more notable is the different shapes of the hardening curves depending on the material direction subjected to uniaxial tension. We note that the specimens subjected to uniaxial tension along the rolling direction show a plateau in the stress-strain curve for true strain between 0.01 and 0.03.

3.2 Incremental measurement of the martensite volume fraction

After extracting small samples from the tensile specimens, micrography (optical metallography) and a global magnetic induction method are used for the measurement of the martensite volume fraction of small samples.

Micrographs are made of unstrained specimens (as-received condition), specimens strained 15% in the material cross direction, and specimens strained 5%, 10%, or 15% in the rolling direction. A micrograph of an as-received specimen is shown in Fig. 3a. Quantitative analysis of the micrographs requires analysis of the grayscale intensity of each pixel in each of the micrographs, following quantitative microscopy guidelines provided in [14].

Differences in preparing the specimen for micrography, including differences between the number of polishing steps used, the concentration of the etchant, the amount of time the etchant is applied, and the technique used to apply the etchant, all result in slightly different micrographs. Because of these variations, different gray scale threshold values, λ_{thresh}, need to be used to differentiate martensite from austenite on different micrographs. However, since the corresponding histograms do not allow for a unique definition of the threshold value (see Fig. 3b), the accuracy of the micrography-based martensite content measurements is very poor. For the micrograph shown in Fig. 3a, a threshold value of λ_{thresh}=120 yields a martensite area fraction of 55%, while a fraction of 70% is obtained for λ_{thresh}=170. Micrography is therefore not a reliable method to quantify the martensite content during tests, nor is it convenient as it requires interrupted tests.

Five samples are extracted from different uniaxial tension specimens and studied using the global magnetic saturation method (sigmameter). This destructive method is very accurate and thus used to calibrate the ferritescope.

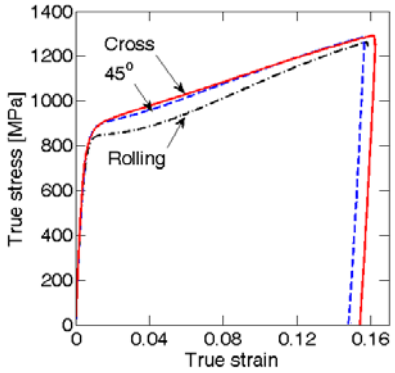

Fig. 2. True stress-strain curves for quasi-static uniaxial tensile loading to 15% strain in three material directions.

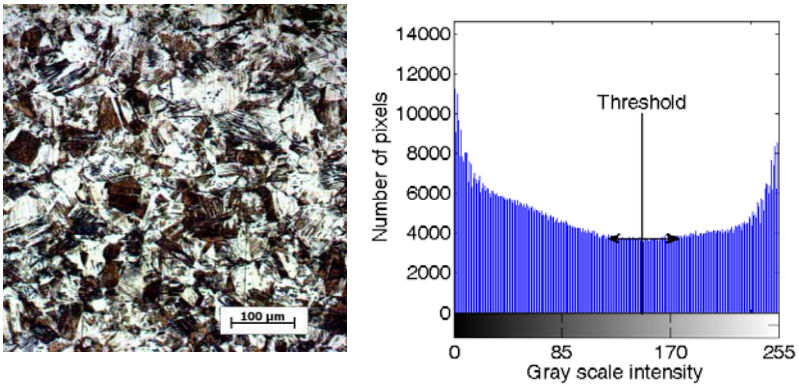

(a) (b)

Fig. 3. Micrograph of (a) specimen in as-received condition. Dark regions indicate martensite while white areas are austenite. Histogram (b) of micrograph in (a) emphasizing the lack of a distinct threshold between grayscale austenite and martensite values.

3.3 Continuous measurement of the martensite volume fraction

The ferritescope reading provides the volume fraction of a magnetic phase by determining the magnetic permeability of the sample with which the ferritescope probe is in contact. In order to ensure that the ferritescope reading does not depend on the orientation of the probe with respect to the material direction, strips that measure 1.5*mm* x 1.5*mm* x 50*mm* are cut with their long dimension aligned with the material rolling direction, the cross direction, and the 45° direction. The ferritescope probe is then placed perpendicular to each 1.5*mm* x 50*mm* plane of each strip, and held in contact with the specimen side. As we vary the configuration such that the probe is aligned with either: the material through-thickness direction, the material cross direction, the material rolling direction, or the material 45° direction, the ferritescope reading does not change. Hence, we conclude that the ferritescope reading does not depend on the material plane to which the probe is perpendicular. In other words, the magnetic permeability may be considered as an isotropic property of the present mechanically-anisotropic sheet material.

The ferritescope is employed in the uniaxial tension tests, and we record the ferritescope signal, S_T, throughout each test. Assuming plastic incompressibility, we calculate the permanent thickness changes based on the axial and width strain recordings. Using Eq. (3) with the calculated thickness, we convert S_T into the thickness-independent ferritescope signal, S_0.

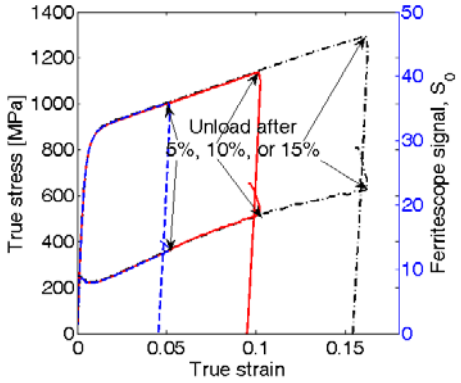

Fig. 4. Stress (upper curves) and thickness-adjusted ferritescope signal (lower curves) versus true strain for uniaxial tension in the material cross direction.

Figure 4 shows the uniaxial tensile stress and the ferritescope signal as a function of the uniaxial strain for specimens strained to 5, 10, or 15% strain in the material cross direction. This plot shows that the ferritescope output signal decreases initially during elastic loading, then increases monotonically during plastic deformation, and increases sharply during elastic unloading. This is known as the Villari effect, in which the material magnetic properties are affected by the elastic strain. Specifically, the magnetic permeability decreases with increasing elastic strain, and as the elastic strain is removed, the magnetic permeability increases until the specimen is in an unloaded state. The decrease in ferritescope signal with increasing elastic strain at the beginning of the test does not indicate reversible phase transformation from martensite to austenite, nor does the increase in ferritescope signal during elastic unloading indicate phase transformation from austenite to martensite during unloading. This plot emphasizes that the specimen must be stress-free for accurate martensite measurements with the ferritescope. To quantify the ferritescope measurement accuracy, we record measurements as we move the probe around the plane of a sheet of metal, in an area of 50x10mm^2, keeping it in contact with the material and perpendicular to the plane of the sheet. The resulting variation of output readings is about +/-5%. The noise in the ferritescope output as the probe is held still at a single point is less than +/-1%.

4. MODELING

The data points in Fig. 5 give the martensite content measured using the ferritescope as a function of von Mises equivalent plastic strain for uniaxial tension specimens strained in three material directions. Santacreu et al. [4] proposed a simple phenomenological transformation kinetics law to describe the deformation-induced martensite formation in stainless steel,

$$\frac{c}{c_{\max}} = 1 - \exp\left\{-[D(\bar{\varepsilon}_0 + \bar{\varepsilon}_{VM})]^n\right\} \tag{4}$$

Because of the apparent isotropic nature of the martensite evolution with plastic strain, we use the von Mises equivalent plastic strain, $\bar{\varepsilon}_{VM}$, as a scalar measure of the deformation in the sheet material. The calibration based on the material data shown in Fig. 5 yields the model parameters $n = 3.5$, $D = 3.7$, $c_{\max} = 100\%$, and $\bar{\varepsilon}_0 = 0.18$. Equation (4) is given as a solid line in Fig. 5. The transformation kinetics may be stress state dependent which requires more advanced transformation laws (e.g. [5]).

We define the yield surface through an equivalent stress $\bar{\sigma}$ and the deformation resistance k,

$$f = \bar{\sigma} - k = 0. \tag{4}$$

Mohr and Jacquemin [15] have shown that the Hill 1948 yield function [16] provides a good approximation of the initial yield surface for the present material. For plane stress conditions, the Hill 1948 equivalent yield stress may be written as

$$\bar{\sigma}_{Hill} = \sqrt{P_{11}\sigma_0^2 + 2P_{12}\sigma_0\sigma_{90} + P_{22}\sigma_{90}^2 + P_{33}\tau^2} \tag{5}$$

where the shape-defining parameter ratios $P_{11}/P_{22} = 1.19$, $P_{12}/P_{22} = -0.46$ and $P_{33}/P_{22} = 2.74$ have been identified based on the biaxial experiments of Mohr and Jacquemin [15]. Note that Eq. (6) defines the von Mises equivalent stress $\bar{\sigma}_{VM}$ when setting $P_{11} = P_{22} = 1.0$, $P_{12} = -0.5$ and $P_{33} = 3.0$. Figure 6 shows both the Hill 1948 and von Mises equivalent stress as a function of the martensite volume fraction for all three experiments. As anticipated from the results of Mohr and Jacquemin [15], the data points lie on top of each other at the beginning of the experiments when using Hill's equivalent stress; the same data show some spread towards the end of the experiments ($c > 80\%$). However, it is interesting to observe that the opposite holds true when plotting the data

in terms of the von Mises equivalent stress, i.e. the differences between the 0°, 45° and 90° experiments become smaller as the martensite content increases. Here, we propose a weighted average of the Hill and von Mises equivalent stresses to define the equivalent stress,

$$\bar{\sigma} = (1 - c^m)\bar{\sigma}_{Hill} + c^m \bar{\sigma}_{VM}. \tag{6}$$

For $c \to 0$ the yield surface shape corresponds to the Hill 1948 surface, while the anisotropy vanishes as the yield surface converges to the von Mises yield surface for a large martensite content ($c \to 1$). The exponent m is introduced to control the yield surface evolution. It is noted that the weighted equivalent stress $\bar{\sigma}$ preserves the degree-one homogeneity of the Hill and von Mises yield functions. The bottom plot in Fig. 6 shows that all data points lie within a narrow band for $m = 2$ and $P_{22} = 1$. Furthermore, we define a linear hardening law $k = k(c)$ for monotonic plastic loading as

$$k(c) = k_0 + Hc \tag{7}$$

with $k_0 = 791MPa$ and $H = 550MPa$ (see solid curve in Fig. 6).

Figure 7 shows the model predictions (solid curves) for uniaxial tension along the 0° and 90° directions. The comparison with the experimentally-measured true stress versus plastic strain curves (dotted curves) demonstrates that the model can describe the distinct change in hardening rate for tension along the rolling direction. At the same time, the asymptotic convergence of the stress-strain curves for large strains is captured by the model. Note that the specific shape of the Hill yield surface is defined through the three parameter ratios given above, while P_{22} may be used to position the Hill surface with respect to the Mises surface. For the special case of $P_{22} = 1$, these two yield surfaces touch each other in the stress space at the point which corresponds to uniaxial tension along the cross-rolling direction. Consequently, the strain hardening along that direction is not affected by the yield surface evolution.

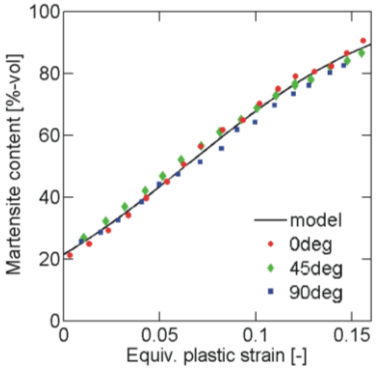

Fig. 5. Evolution of the martensite volume fraction during uniaxial experiments as a function of von Mises equivalent plastic strain.

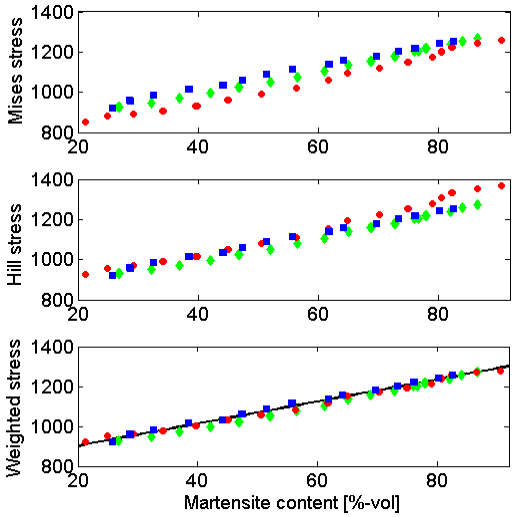

Fig. 6. Deformation resistance as a function of the martensite volume fraction for specimens loaded along the 0° (red), 45° (green) and 90° (blue) directions. The results are shown for different equivalent stress definitions (von Mises stress = top; Hill'48 stress = middle, weighted average stress = bottom).

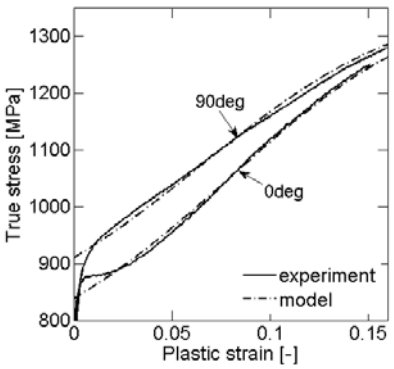

Fig. 7. Comparison of the model predictions (dashed curves) with the experimentally-measured stress-strain curves (solid curves) for uniaxial tension along the rolling direction (0deg) and transverse direction (90deg).

5. SUMMARY

A ferritescope has been calibrated based on magnetic saturation induction measurements to monitor the martensite content evolution throughout uniaxial tensile experiments. Both X-ray diffraction and optical metallography did not provide satisfactory measurement accuracy. The results show that the Villari effect may lead to major errors during in-situ ferritescope measurements. Therefore, the specimens are periodically unloaded throughout each test to determine the magnetic permeability under stress-free conditions.

Previous studies have shown that the kinetics of the austenite-to-martensite transformation in metastable stainless steels are stress-state dependent (e.g. [5]), and the ferritescope can now be used throughout biaxial experiments [17] to provide an experimental basis for the development of stress-state dependent martensitic transformation laws. Furthermore, Mohr and Jacquemin [15] have recently shown that stainless steels feature non-associated anisotropic hardening, i.e. the strain hardening under monotonic loading cannot be described by a single equivalent stress versus work-conjugate equivalent plastic stress curve. Here, we have performed in-situ martensite content measurements throughout uniaxial tensile tests to demonstrate that the initial texture has no measurable effect on the martensitic phase transformation kinetics. The initial texture causes anisotropy in the strain hardening response, while the evolution of the martensite content appears to be direction independent.

The authors are grateful to the partial support of the MIT Fracture Consortium on Advanced High Strength Steels as well as a U.S. Department of Defense National Defense Science and Engineering Graduate Fellowship. Thanks are due to Benoit Proult of ArcelorMittal for valuable discussions and their help on the martensite content measurements. Thanks are also due to Dr. Scott Speakman of MIT for assistance with X-ray diffraction analysis. This work made use of the MRSEC Shared Experimental Facilities supported by the National Science Foundation under award number DMR - 0819762.

References

[1] T. Angel. J Iron Steel Inst, 177, p. 165 (1954)
[2] F. Lecroisey, A. Pineau. Metall Trans, 3(2), p. 387 (1972).
[3] G.B. Olson, M. Cohen. Metall Matls Trans A, 6(3), p. 791 (1975).
[4] P.O. Santacreu, J.C. Glez, G. Chinouilh, T. Frohlich. Steel Res Int 77(9-10), p. 714 (2006).
[5] R.G. Stringfellow, D.M. Parks, G.B. Olsen. Acta Metallurgica, 40(7), p. 1703 (1992).
[6] J. Post, H. Nolles, K. Datta, H.J.M. Geijselaers. Matls Sci Engng A, 498, p. 179 (2008).
[7] M. Smaga, F. Walther, D. Eifler. Matls Sci Engng A, 483-484, p. 394 (2008).
[8] J. Talonen, P. Aspegren, H. Hanninen. Matls Sci Tech, 20(12), p. 1506 (2004).
[9] L. Zhao, N.H. van Dijk, E. Bruck, J. Sietsma, S. van der Zwaag. Matls Sci Engng A, 313(1-2), p. 145 (2001).
[10] E. Beraha, B. Spigher. Amer Soc Metals, p. 20 (1977).
[11] ASTM standard A894/A894M (2005).
[12] G.W. Greenwood, R.H. Johnson. Proc Roy Soc A283, p. 403 (1965).
[13] Fischer Feritscope MP30E-S Operator's Manual, Version 2.2 (2006).
[14] American Society for Metals, Metals Handbook: Metallography, Structures and Phase Diagrams, 8th Edition, Vol. 8, Metals Park, Ohio: American Society for Metals (1973).
[15] D. Mohr, J. Jacquemin. J Mech Phys Solids 56(10), p. 2935 (2008).
[16] R. Hill. Proc Roy Soc A, 193(1033), p. 281 (1948).
[15] D. Mohr, M. Oswald. Exp Mech, 48(1), p. 65 (2008).